Improvement on a Michelson interferometer for bunch length measurement of a femtosecond accelerator

LIN Xuling[1,2,*] ZHANG Jianbing[1] BEI Hua[1,2] DAI Zhimin[1]

[1] *Shanghai Institute of Applied Physics, Chinese Academy of Sciences, Shanghai 201800, China*

[2] *Graduate School of Chinese Academy of Sciences, Beijing 100049, China*

Abstract Based on the femtosecond accelerator facility at Shanghai Institute of Applied Physics (SINAP), a conventional far-infrared Michelson interferometer was built to measure the bunch length by means of optical autocorrelation. However, according to the preliminary experiment result, the resolution of interferometer is not good enough, because the mirror-driving mechanism makes the moving mirror tend to tilt or wobble as it retards. Considering of the allowable errors, we calculate the maximum allowable titling angle of the moving mirror, and discuss the alignment plan in this paper.

Key words Coherent transition radiation, Bunch length, Interferometer, Dynamic alignment

1 Introduction

The ability to measure sub-picosecond electron bunches determines progresses in producing ultra short pulses of electrons and radiations for future linear colliders, X-ray FELs or development of far infrared (FIR) coherent radiations of very high intensity[1]. Coherent transition radiation (CTR), emitted by electron bunches upon crossing a thin aluminum foil, is a promising method to diagnose sub-picosecond electron beam bunches[2]. If wavelength is longer than the bunch length, the radiation is coherent and the radiation intensity is proportional to the square of the number of electrons per bunch. The spectral intensity emitted by a bunch of N particles takes the form as

$$I_{\text{tot}}(\omega) = NI_1(\omega) + N(N-1)I_1(\omega)\left|f(\omega)\right| \quad (1)$$

where $I_1(\omega)$ is the intensity radiated by a single electron and $f(\omega)$ is the bunch form factor[3,4], which is the Fourier transform of the normalized electron density distribution ρ, For a relativistic bunch whose transverse dimensions is smaller than the length, the form factor becomes

$$f(\omega) = \int \rho(z) exp(i\omega z / c)dz = \int c\rho(ct) exp(i\omega t)dt \quad (2)$$

By measuring the radiation spectrum, one obtains the form factor and electron density distribution through Fourier transform. This is often done by examining the autocorrelation of CTR signals with a Michelson interferometer[5] to obtain the amplitude of the beam current's Fourier transform.

A far-infrared Michelson interferometer has been used in bunch length measurements of a femtosecond accelerator at SINAP. However, resolution of the interferometer is not as good as we expected due to its misalignment. For a Michelson interferometer, better resolutions can be achieved by maximizing the optical path difference between two parts of the coherent light, when the mirrors remain in good alignment throughout the entire scan and the light passing the interferometer is sufficiently collimated. In this paper, a precise and relatively simple alignment method and an alignment system are developed.

2 Experimental

The femtosecond accelerator consists of mainly a thermionic RF gun, an α magnet to compress electron bunches produced by the RF gun, and a SLAC type accelerating tube. The beam bunches are transported to

Supported by Major State Basic Research Development Program of China (2002CB713600)

* Corresponding author. *E-mail address:* linxuling@sinap.ac.cn

Received date: 2008-11-25

the linac to accelerate then to 20–30 MeV (Fig.1). Coherent radiations are generated in the form of transition radiation when the electrons pass through an interface between two media of different dielectric constants[6]. By placing an aluminum foil as a radiator in the electron path, transition radiation is emitted at the foil-vacuum interfaces. As shown in Fig.2, an Al-foil is placed by 45° to the beam incidence and the transition radiation is emitted perpendicular to the beam incidence. The divergent radiations exit through a quartz window, and are converted to a quasi-parallel beam by an off-axis parabolic mirror.

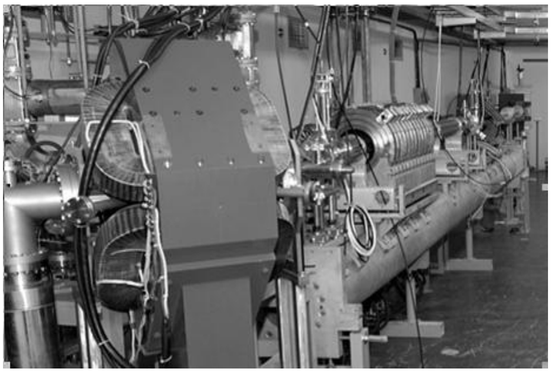

Fig.1 Plot of the device layout.

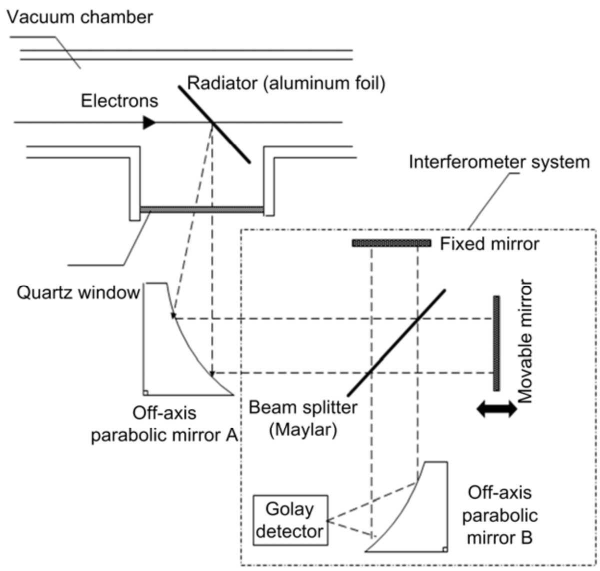

Fig.2 Schematic diagram of the experimental setup to measure bunch length using coherent transition radiation in a Michelson interferometer. The aluminum foil is the transition radiation radiator, and the crystalline quartz window and off-axis parabolic mirror A are used to transport the radiation to the interferometer.

The far-infrared Michelson interferometer shown in Fig.3 is composed of a beam splitter, a fixed mirror and a movable mirror. A light beam entering the interferometer is split into two parts by the beam splitter. The two parts traveling in two directions are reflected back by the mirrors. Then, the two radiation pulses combine and transmit into a Golay detector to measure the light intensity. Preliminary measurement result of the interferogram are shown in Fig.4[7].

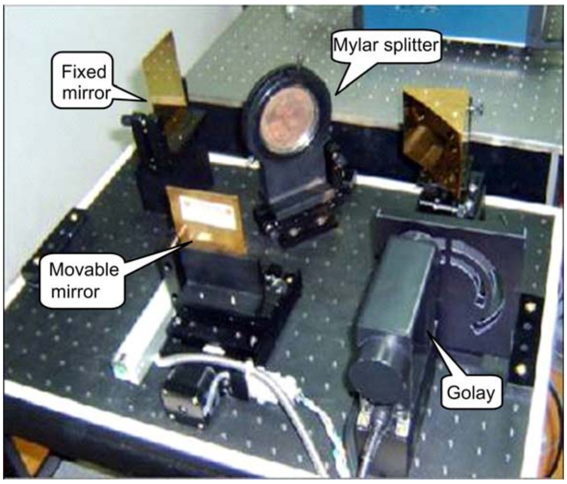

Fig.3 Actual picture of far-infrared Michelson interferometer at hand.

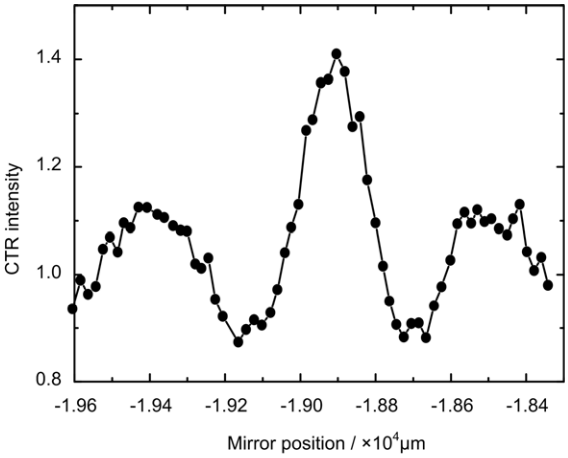

Fig.4 Interferogram from a bunch length measurement.

3 The maximum allowable mirror tilting

The precision of spectra measured by the Michelson interferometer depends both on the alignment of the fixed mirror relative to the moving mirror and on how accurately the moving mirror's plane is maintained during the scan[8]. For producing the interferograms used for spectroscopic analysis, the two lights must converge at the same point on the beam splitter. However, the moving mirror tends to tilt or wobble as it is retarded and, as a result, will not be perpendicular to the incident light all the time. This causes the light reflected by the movable mirror to deviate off the optical axis of the detector (Fig.5).

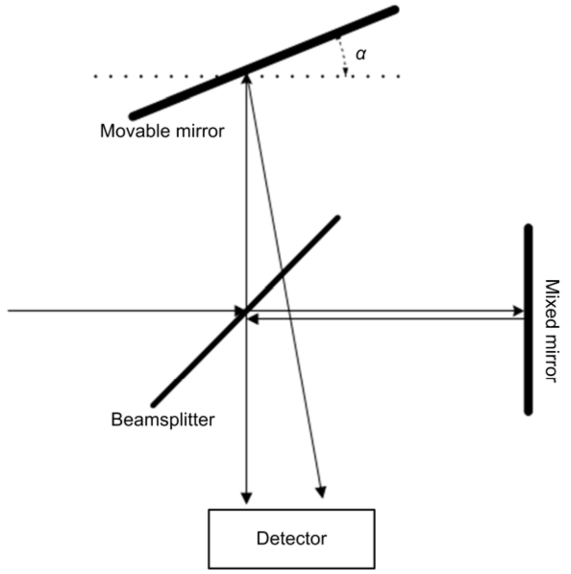

Fig.5 Schematic diagram of the Michelson's optics showing how tilting the moving mirror causes the recombinant beams to diverge from the optical axis.

To calculate the maximum allowable mirror tilting, we introduce the modulation efficiency for a circular light spot on the mirrors. It can be written as

$$\eta(m) = 2\times[J_1(a)/a] \tag{3}$$

where $\eta(m)$ is the modulation efficiency, $J_1(a)$ is the first order Bessel function of a, which is described by

$$a=4\pi\sigma\alpha r \tag{4}$$

where σ is frequency of interest (cm^{-1}), α is the tilting angle (radians), and r is radius of light spot (cm).

As a general rule, satisfactory modulation efficiency must be[9]

$$\eta(m) \ge 0.9 \tag{5}$$

$$2\times[J_1(a)/a] \ge 0.9 \tag{6}$$

According to Cohen[10], Eq.(3) can be approximated by

$$\frac{2J_1(4\pi\sigma r\alpha)}{4\pi\sigma r\alpha} \approx 1 - A\sigma^2\alpha^2 \tag{7}$$

Assuming σ=100 cm^{-1}, r=2.5 cm, the allowable mirror tilting can be maintained at $\alpha \le 2.85\times10^{-4}$ radians, or $\alpha \le 58.7$ arc seconds.

4 The design of alignment method

It is a tough task to achieve α<58.7 arc seconds throughout the scan. Most of the translation stages available to carry the mirror cannot meet such high straightness requirement. Therefore, we can have two choices in designing the interferometer. [11,12]. The first is the cat eye or corner cube reflectors, which in turn must be individually aligned to a high precision and maintained at the component-subassembly level. The second choice is a dynamically aligned system with inherent design robustness and ability to carry out self alignment. We chose the second solution.

Several dynamic alignment methods have been developed for interferometer in infrared region[13-16]. However, complicated optical-electrical servo and mechanical system are used in those systems. Instead, we developed a relatively simple dynamic alignment system for a scanning Michelson interferometer in the THz wavelength range.

A schematic diagram of the dynamic alignment interferometer system is shown in Fig.6. An expanded He-Ne laser beam goes into the interferometer collinearly with the THz light. After being modulated by the interferometer, the laser beam projects on the detector board consisting of three detectors (Fig.7).

If the plane of the moving mirror remains parallel throughout the scan, the optical path differences for the three detectors will be equal, and signals from the detectors will be in phase. Tilting the moving mirror causes phase differences between the three detectors. Detector A is at the centre of the mirror. Detectors B and C are placed in such a way that $\overline{AB}=\overline{AC}=R$ and $\overline{AB} \perp \overline{AC}$, where $\overline{AB}$ denotes the straight lines between A and B, and $\overline{AC}$ between A and C. The relationship between the phase difference and tilting angle is given by[10]

$$\Delta\varphi_{\mathrm{AC}} = 4\pi\times\frac{R}{\lambda}\times\alpha \tag{8}$$

$$\Delta\varphi_{\mathrm{AB}} = 4\pi\times\frac{R}{\lambda}\times\beta \tag{9}$$

where $\Delta\varphi_{\mathrm{AC}}$ is the phase difference between Detectors A and C, $\Delta\varphi_{\mathrm{AB}}$ is the phase difference between detectors A and B, and α and β are the tilting angle. A phase detection circuit deals with the output wave of the detector, picking up the phase differences of $\Delta\varphi_{\mathrm{AC}}$ and $\Delta\varphi_{\mathrm{AB}}$ then sent phase data to DSP processor. The DSP processor runs the control algorithm and calculates the tilting angle, which in turn is used to control the piezo-ceramic actuators that placed under one of the mirrors and allow for tilt correction.

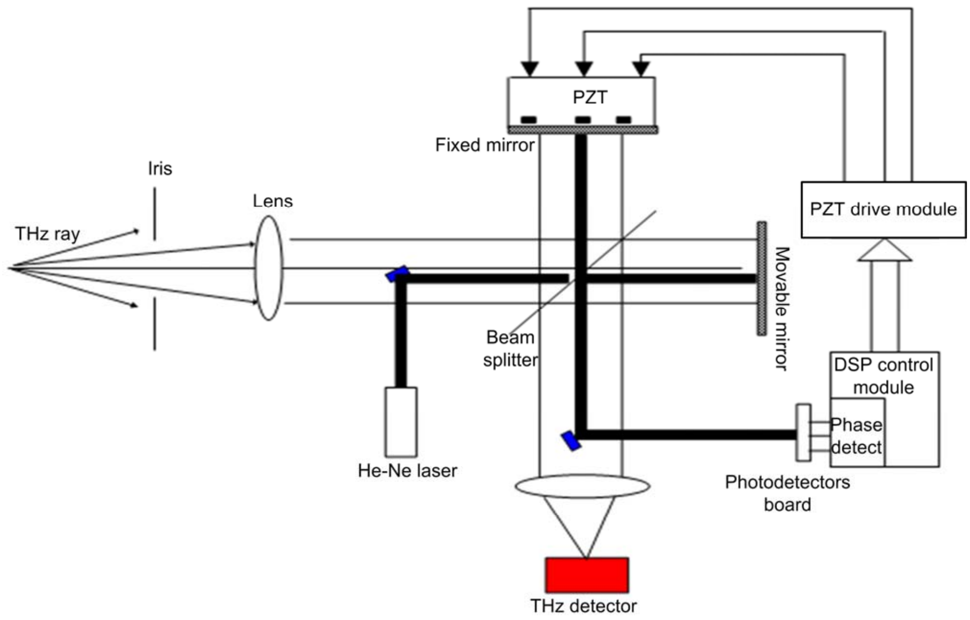

Fig.6 Schematic diagram of dynamic alignment Michelson interferometers.

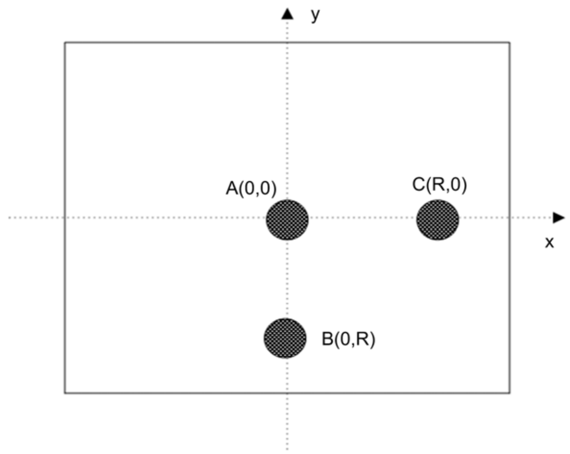

Fig.7 Detector board of the He-Ne laser.

5 Conclusions

According to the preliminary experiment result, we analyzed the error of mirror tilting in the interferometer. Base on the error analysis, the max tilting angle is calculated, and the alignment plan is given. We are to purchase relevant subassemblies and improve the interferometer. We believe that better resolutions will be obtained in our measurement of the bunch length.

Reference

1 Edwards D A, TESLA test facility linac design report, Hamburg: DESY-TESLA, 1995, **01:** 01–09.

2 Happek U, Sievers A J, Blum E B. Phys Rev Lett, 1991, **67:** 2962–2965.

3 Lai R, Sievers A J. Nucl Instrum Method A, 1997, **397:** 221–231.

4 Lai R, Sievers A J. Phys Rev E, 1995, **52:** 4576–4579.

5 Lihn H C, Kung P, Settakorn C, Weidemann H. Phys Rev E, 1996, **53:** 6413–6418.

6 Liu A Q. Generation of terahertz CTR/CDR and its application for bunch measurement, Shanghai: Shanghai Institute of Applied Physics, 2005, 61–76.

7 Gu Q, Chen Y Z, Dai Z M, *et al.* High power laser and particle beam, 2008, **20:** 585–588.

8 Griffiths Peter R, James A.de Haseth, Fourier transform infrared spectrometry (2nd ed.). Hoboken: Wiley-Interscience, 2007, 47–50.

9 Xiang L B, Yang J F. Acta Photonica Sin, 1997, **26:** 132–135 (in Chinese).

10 Cohen D. Appl Opt, 1997, **36:** 4034–4042.

11 Yin B S, *et al.* Opt Instrum, 2006, **28:** 74–79 (in Chinese).

12 Yu L M, Dai Z X. Infrared, 2002, **39:** 18–22 (in Chinese).

13 Lu Z J, Koehler R A, Gault W A, *et al.* J Phys E: Sci Instrum, 1988, **21:** 71–74.

14 Morrison E, Meers B J, Robertson D I, *et al.* Appl Opt, 1994, **33:** 5041–5049.

15 Barone F, Milano L, Russo S, *et al.* IEEE Trans Nucl Sci, 1992, **39:** 232–237.

16 Goldberg K A, Naulleau P, Bokor J. Appl Opt, 2002, **41:** 4477–4483.